POSTURE MATCHING AND ELASTIC REGISTRATION OF A MOUSE ATLAS TO SURFACE TOPOGRAPHY RANGE DATA

A. A. Joshi[1], A. J. Chaudhari[2], Changqing Li[2], D. W. Shattuck[1], J. Dutta[3], R. M. Leahy[3] and A. W. Toga[1]

[1]Laboratory of Neuro Imaging, UCLA School of Medicine, Los Angeles, CA 90095, USA,
[2]Department of Biomedical Engineering, University of California-Davis, Davis, CA 95616, USA,
[3]Signal and Image Processing Institute, University of Southern California, Los Angeles, CA 90089, USA

ABSTRACT

Estimation of internal mouse anatomy is required for quantitative bioluminescence or fluorescence tomography. However, only surface range data can be recovered from all-optical systems. These data are at times sparse or incomplete. We present a method for fitting an elastically deformable mouse atlas to surface topographic range data acquired by an optical system. In this method, we first match the postures of a deformable atlas and the range data of the mouse being imaged. This is achieved by aligning manually identified landmarks. We then minimize the asymmetric L^2 pseudo-distance between the surface of the deformable atlas and the surface topography range data. Once this registration is accomplished, the internal anatomy of the atlas is transformed to the coordinate system of the range data using elastic energy minimization. We evaluated our method by using it to register a digital mouse atlas to a surface model produced from a manually labeled CT mouse data set. Dice coeffices indicated excellent agreement in the brain and heart, with fair agreement in the kidneys and bladder. We also present example results produced using our method to align the digital mouse atlas to surface range data.

Index Terms— Deformable atlas, mouse registration, optical tomography

1. INTRODUCTION

Anatomical atlases with appropriate co-registration schemes can be useful tools for small animal studies involving modalities that are incapable of imaging anatomy. Specifically, in optical fluorescence tomography (OFT) and bioluminescence tomography (BLT) studies in small animals, where estimation of the internal organ optical properties via all-optical techniques is non-trivial [1], deformable anatomical atlases may be used with published optical properties [2]. The atlas must first be aligned with the optical images of the individual mouse being studied.

In optical studies, anatomical images such as those from computed tomography (CT) or magnetic resonance imaging (MRI) are often not acquired due to the inavailability of the scanners in the same facility, concerns such as radiation dose in case of CT, viability and associated cost [3]. The surface geometry of the animal can be estimated using optical systems [4, 5]. These systems typically produce a height map of the animal consisting of discrete points (called range data), contours, or silhouettes that can then be used to generate a 3D representation of the animal volume. For a finite element method (FEM) based solution to the diffusion equation of light propagation, a volumetric tessellation of the animal needs to be generated for the surface map [6]. This process is non-trivial since these range data are often incomplete or under-sampled [7]. Minimization of commonly used symmetric distance metrics such as L^2 or Hausdorff distance [8] is not suitable when the measured range data are incomplete. Asymmetric L^2 pseudo-distance minimization between the two data offers an attractive alternative since the local minima will occur when incomplete surface range data match with part of the complete data set.

In this paper, we present a volumetric registration scheme that warps the Digimouse atlas [9] to an optically-imaged mouse based only on the atlas data and the measured surface topography of the imaged animal. We achieve this registration in three stages:

1) The Digimouse is repositioned and its posture is corrected to match the position and posture of the mouse in the acquired data set.
2) The posture-corrected atlas is then warped to the available surface topographic data using the asymmetric L^2 pseudo-distance.
3) The internal anatomy data in the warped atlas is transformed corresponding its deformed surface. The volumetric tessellation is also transformed using the computed deformation field.

We performed a validation of our method based on micro-CT data acquired from the optically imaged animal.

2. MATERIALS AND METHODS

2.1. The Digimouse atlas

We used the Digimouse atlas [9] as our anatomical template. The Digimouse was generated using co-registered CT and cryosection images of a 28g normal male nude mouse. Seventeen anatomical structures were labeled in the Digimouse. A corresponding volumetric tetrahedral mesh was provided by the Digimouse atlas. It was generated using the constrained-Delaunay method which conforms to organ boundaries. This mesh contains $N = 58,244$ vertices and $T = 306,773$ tetrahedral faces.

2.2. Deformable elastic modeling of the Digimouse

We model the atlas mouse body as an elastic volume (Ω) and therefore, deformations to it will be governed by the elastic equilibrium equation, i.e. at equilibrium, the elastic energy $L(u)$ corresponding to deformation u equals the external forces f applied on the body [10]:

$$L(u) = f = -\text{div}\left[(I + \nabla u)\,\hat{S}\right] \quad \hat{S} : \Omega \to \mathbb{R}^3, \quad (1)$$

where $\hat{S}$ denotes the second Piola-Kirchoff stress tensor defined by $\hat{S} = \lambda\text{Tr}(\hat{G})I + 2\mu\hat{G}$ with $\hat{G} = \frac{1}{2}(\nabla u^T + \nabla u + \nabla u^T \nabla u)$ representing the Green-St. Venant strain tensor. The coefficients λ and μ are Lamé's elastic constants. Linearization of (1) using Fréchet derivatives leads to

$$L(u) = -\text{div}(S) = f, \quad (2)$$

where, $S = \lambda\text{Tr}(G) + 2\mu G$ is the linearized stress tensor and $G = \frac{1}{2}\left(\nabla u + \nabla u^T\right)$ is the linearized strain tensor [10]. The elasticity operator L is discretized using a finite element method. In brief, the equilibrium equation in (2) is formulated by using a variational principle in an energy minimization, which leads to a quadratic form $U^T K U$, where $U = [U_1, U_2 ..., U_N]^T$ is the vector of displacements at N nodes in the tetrahedral mesh. The matrix K uses FEM to discretize the elastic energy operator. When external forces are applied at the surface points such that the surface points $U_i, \{i \in \partial\Omega\}$ transform to their new locations V_i, the elastic energy becomes

$$E_{elastic}(U) = U^T K U + \alpha \sum_{i \in \partial\Omega} \|U_i - V_i\|^2, \quad (3)$$

where $\alpha > 0$ is a mismatch penalty parameter.

This mathematical formulation allows the whole mouse atlas volume deform elastically when displacements are applied on only the surface nodes of its mesh. The external forces in this formulation are non-zero at the mouse surface $\partial\Omega$ and will be used to guide the volumetric deformations in section 2.3 and section 2.4.

2.3. Posture correction

There are a wide variety of postures in which mice are imaged at various imaging facilities since a standard has not been established. Typically, the positions of limbs, the position of
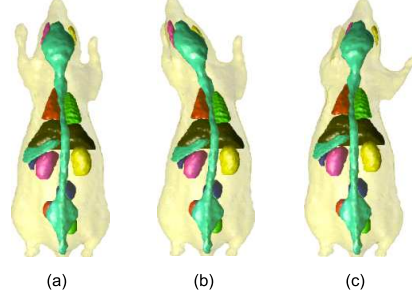
Fig. 1. Posture correction for the Digimouse: (a) the Digimouse, (b) a different orientation of the head, (c) a different orientation of the head and the right fore limb.

the head and the orientation of the animal vary greatly. As an initial step, the limbs and head of the Digimouse need to be repositioned to match those of the mouse being imaged. We used a landmark-based method with the elastic mouse model from section 2.2 for posture correction. We selected five landmarks, denoted here by $p_i \in \partial P, i \in 1, \cdots, 5$ on the surface $\partial\Omega$: one each at the ends of the four limbs and one at the center point on a line connecting the two ears. Corresponding landmarks $a_i \in \partial\Omega, i \in 1, \cdots, 5$ were also selected on the atlas. This gave five displacement vectors $W_i = (p_i - a_i)$ at the atlas surface points a_i. The displacement vector field was then extrapolated to the whole mouse surface $\partial\Omega$ by minimizing the Sobolev energy:

$$E_s(U) = ||\Delta_d U||^2 + \beta \sum_{i=1}^{5} (U_i - W_i)^2, \quad (4)$$

where Δ_d denotes the discretized Laplacian operator matrix for the atlas surface $\partial\Omega$ [11] and $\beta > 0$ is a mismatch penalty parameter. Let the vector $U_s^p : \{s \in \partial\Omega\}$ be the minimizer of the energy in (4) and $\partial\Omega^d = \partial\Omega + U^p$ denote the warped atlas surface. Then, we use the elastic mouse model from section 2.2 to warp the internal anatomy of the mouse. The elastic energy minimization in (3):

$$E_{elastic}(U) = U^T K U + \alpha \sum_{s \in \partial\Omega} (U_s - U_s^p)^2 \quad (5)$$

leads to a displacement field U^p at the volumetric points, that when applied to the atlas Ω, leads to a warping of the internal organs consistent with the warped surface. The posture-corrected atlas is now given by $\Omega_p = \Omega + U^p$. Sample postures of Digimouse obtained using this procedure are shown in the Fig. 1.

2.4. Surface fitting and elastic volume warping

In order to be able to register the surface topography data recovered from the optical setup to the atlas surface, the matching problem is formulated as an asymmetric L^2 pseudo-distance minimization, where the distance is computed from the incomplete surface to the complete surface. We define the asymmetric L^2 pseudo-distance metric d between an incomplete acquired surface ∂P and the posture-corrected atlas

surface $\partial \Omega_p$ by:

$$d(\partial \Omega_p, \partial P) = \sum_{p \in \partial P} \left(\inf_{e \in \partial \Omega} \|p - e\|^2 \right). \qquad (6)$$

Our objective, then, is to deform the posture matched atlas surface $\partial \Omega_p$ from section 2.3 such that the distance metric in (6) is minimized. Additionally, we want the displacement field for this operation U^s to be smooth, such that the deformed surface $\partial \Omega_p + U^s$ remains smooth. This is achieved by a Laplacian regularizer on the displacement field. Due to this regularizer, the cost function C_S is in the form of a Sobolev norm and is given by:

$$C_S(U) = \sum_{p \in P} \left(\inf_{e \in \partial \Omega} d(p, a + U_e) \right)^2 + \|\Delta_d U\|^2 \qquad (7)$$

where Δ_d denotes the discrete Laplacian [11]. The minimization of the pseudo-distance is performed by a searching strategy over the point-set and results in a displacement vector U^s. The displacement field U^s obtained as a result of this minimization is then applied to the posture-corrected atlas surface $\partial \Omega_p$ to get the surface $\partial \Omega_m = \partial \Omega_p + U^s$ that matches with the range data ∂P.

Similar to section 2.3, the surface warp is then extrapolated to the entire mouse volume using the elastic mouse model. Then, the energy minimization in (3):

$$E_{elastic}(U) = U^T K U + \alpha \sum_{s \in \partial \Omega_p} (U_p - U_p^s)^2 \qquad (8)$$

leads to a displacement field U^m at the volumetric points that, when applied to the posture-corrected atlas Ω_p, leads to a warping of the internal organ labels consistent with the warped surface $\partial \Omega_s$. Thus, the posture-corrected atlas is given by $\Omega_s = \Omega_p + U^m$. The result is a warped mouse atlas Ω_s with the surface $\partial \Omega_s$ conforming to the range data ∂P.

2.5. Implementation of the warping method
The warping method was implemented in MATLAB®. The conjugate gradient minimization procedure was used for the cost function minimizations in sections 2.3 and 2.4. We empirically chose Young's modulus = 1 and Poisson ratio = 0.3 for computing the elasticity matrix K [12], $\alpha = 3, \beta = 1$.

2.6. Micro-CT acquisition and labelling for evaluation
A micro-CT scan of an anesthetized normal adult mouse (nu/nu, weight = 26 g) was acquired using the MicroCAT II scanner (Siemens Preclinical Solutions, Knoxville, TN). The experiment was performed under a protocol approved by the University of California - Davis Animal Care and Use Committees. We extracted the mouse surface from the CT image using BrainSuite's [13] mask tool and surface generation tool. We manually erased the nose cone from the binary mask. This mouse surface served as a target topography surface ∂P for evaluation. The brain, the heart, the two kidneys and the bladder were segmented manually by an experienced observer using BrainSuite [13].
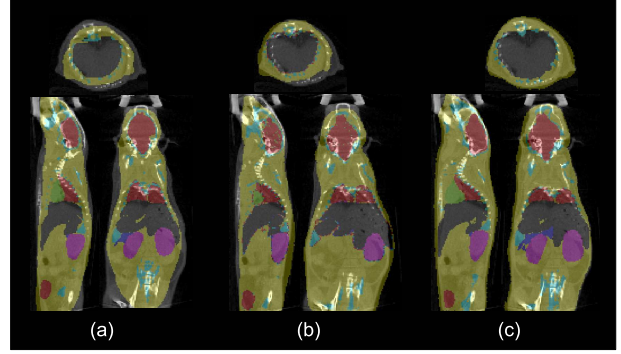
Fig. 2. Results from the performance evaluation study. In each case, three orthogonal sections from the CT scan of the target are overlaid with the corresponding sections of the Digimouse (a) after only rigid registration, (b) after posture-correction and, (c) after the asymmetric L^2 distance-based method were used.

2.7. Acquisition of surface topographic range data
Our surface profiling scheme used a conical mirror with a horizontal stage that held the animal in an axial orientation within it [14]. A normal anesthetized adult mouse (nu/nu, weight = 24 g) was used for this experiment. The dorsal portion of the animal was scanned by the three line-laser setup. Using geometrical optics formulae, and by translating the laser source horizontally, the complete animal was scanned. The complete procedure lasted 25 min. No data were acquired for the ventral surface.

3. RESULTS

3.1. CT-based evaluation
We used the mouse surface extracted from the CT scan as our target surface. We matched the posture of the Digimouse atlas to that of the target animal using the procedure described in section 2.3. This produced a repositioned and posture-matched atlas. The warping field generated for the tetrahedral mesh was used to resample the labeled CT of the Digimouse using nearest neighbor interpolation. An overlay of the warped labels and the mouse CT is shown in figure 2(b). The asymmetric L^2 pseudo-distance based minimization described in section 2.4 lead to an improved surface and volume warping shown in figure 2(c). The whole method took approximately $20 - 30$ min of runtime on a Pentium IV 3.6 GHz machine with 4GB RAM.

We compared the accuracy of our method by computing Dice coefficients [15] of set overlap between warped atlas labels and manually determined labels for the brain, the heart, the two kidneys and the bladder. Our results are tabulated in Table 1.

3.2. Performance evaluation for range data from an optical scan
Range data were acquired using the optical technique described in section 2.7. Figure 3(a) shows the point cloud

Organ name	Dice Coefficient= $\frac{2|A \cap B|}{|A|+|B|}$
Brain	0.8273
Heart	0.8161
Kidneys	0.5899
Bladder	0.5481

Table 1. Dice coefficients of organ overlap between warped atlas labels (A) and manually assigned labels (B)

(a)   (b)   (c)   (d)
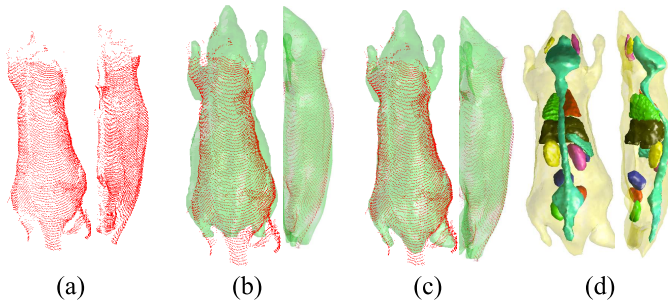
Fig. 3. Estimation of internal anatomy for optical data: (a) the point cloud obtained from the optical scan, (b) the point cloud and the posture-corrected Digimouse, (c) the point cloud and the final result of surface fitting by our scheme, (d) elastically transformed animal volume whose surface fits the point cloud.

representing the top surface of the animal. Figure 3(b) shows an overlay of the point cloud on the posture-corrected Digimouse surface (shown in green). This warping is further improved by the asymmetric L^2 distance minimization procedure to obtain the results in figure 3(c). The internal organs were then elastically warped using the surface as a guide to produce figure 3(d).

4. DISCUSSION AND CONCLUSIONS

We have presented a deformable mouse atlas based registration scheme for estimating internal anatomy of an animal when only surface topography information is available. We evaluated our proposed scheme against results from an anatomical imaging modality. For the heart and the brain, high Dice coefficients between the anatomical image and the warped atlas imply that the head and the chest region of the warped atlas had excellent alignment even though only surface information was used. The bladder and kidneys show significant shape variability across subjects but overlap metric greater than 50% were achieved using the proposed method, even in these regions. The proposed scheme could allow detailed investigation of anatomical variability on optical source reconstruction and facilitate comparisons with methods that derive anatomical information from all-optical techniques. Additionally, the organ map derived from the proposed method can serve as an anatomical prior for diffuse optical tomography.

Exact alignment of mouse surfaces is not enforced in our

method since we wanted the deformation of the atlas surface to be smooth. Thus, we have a Sobolev regularizing term in the matching energy equation (4). This term tends to avoid fold-overs in the deformed surface and leads to topologically correct deformations of the mouse atlas. Quasi-rigid and bending priors can be enforced in our method. Such priors allow rigid movement of the bones and the skeleton while still relaxing the rigidity constraints for other organs. In cases where internal anatomical information is available, our proposed method can provide a good initialization for atlas-based registration. Additionally, the proposed method can provide a good initialization for segmentation in cases where an intensity-based anatomical image such as CT or MR is available.

5. REFERENCES

[1] A. P. Gibson, J. C. Hebden, and S. R. Arridge, "Recent advances in diffuse optical imaging," *Phys Med Biol*, vol. 50, no. 4, pp. R1–43, 2005.

[2] G Wang, W Cong, K Durairaj, X Qian, H Shen, P Sinn, E Hoffman, G McLennan, and M Henry, "In vivo mouse studies with bioluminescence tomography," *Optics Express*, vol. 14, no. 17, pp. 7801–7809, 2006.

[3] V. Ntziachristos, E.A. Schellenberger, J. Ripoll, D. Yessayan, E. Graves, A. Bogdanov, L. Josephson, and R. Weissleder, "Visualization of antitumor treatment by means of fluorescence molecular tomography with an annexin V-Cy5. 5 conjugate," *Proceedings of the National Academy of Sciences*, vol. 101, no. 33, pp. 12294–12299, 2004.

[4] J. Ripoll, R. B. Schulz, and V. Ntziachristos, "Free-space propagation of diffuse light: theory and experiments," *Phys Rev Lett*, vol. 91, no. 10, pp. 103901, 2003.

[5] Bradley W. Rice, Heng Xu, and Chaincy Kuo, "Surface construction using combined photographic and structured light information," May 2006, Patent Application 0268153.

[6] M. Schweiger, SR Arridge, and DT Delpy, "Application of the finite-element method for the forward and inverse models in optical tomography," *Journal of Mathematical Imaging and Vision*, vol. 3, no. 3, pp. 263–283, 1993.

[7] H. Hoppe, T. DeRose, T. Duchamp, J. McDonald, and W. Stuetzle, "Surface reconstruction from unorganized points," *Computer Graphics*, vol. 26, pp. 71–78, 1992.

[8] I. Eckstein, J.P. Pons, Y. Tong, C.C.J. Kuo, and M. Desbrun, "Generalized Surface Flows for Mesh Processing," in *Symposium on Geometry Processing*, 2007, pp. 183 – 192.

[9] B. Dogdas, D. Stout, A. F. Chatziioannou, and R. M. Leahy, "Digimouse: a 3D whole body mouse atlas from CT and cryosection data," *Phys Med Biol*, vol. 52, no. 3, pp. 577–87, 2007.

[10] G. Postelnicu, L. Zollei, and B. Fischl, "Combined volumetric and surface registration," *Medical Imaging, IEEE Transactions on*, 2008, accepted.

[11] M.K. Chung, S.M. Robbins, K.M. Dalton, R.J. Davidson, A.L. Alexander, and A.C. Evans, "Cortical thickness analysis in autism with heat kernel smoothing," *Neuroimage*, vol. 25, no. 4, pp. 1256–1265, 2005.

[12] T.J.R. Hughes, *The finite element method*, Prentice-Hall, 1987.

[13] D.W. Shattuck and R.M. Leahy, "BrainSuite: An automated cortical surface identification tool," *Medical Image Analysis*, vol. 6, no. 2, pp. 129–142, 2002.

[14] Changqing Li, Gregory S. Mitchell, Joyita Dutta, Sangtae Ahn, Richard M. Leahy, and Simon R. Cherry, "A three-dimensional multispectral fluorescence optical tomography imaging system for small animals based on a conical mirror design," *Opt. Express*, vol. 17, no. 9, pp. 7571–7585, 2009.

[15] CJ Van Rijsbergen, *Information Retrieval*, Butterworth-Heinemann Newton, MA, USA, 1979.